polymer papers

Dimensions of crystallites in a thermotropic random copolyester

S. Hanna, T. J. Lemmon*, R. J. Spontak† and A. H. Windle‡
Department of Materials Science and Metallurgy, University of Cambridge, Pembroke Street, Cambridge, CB2 3QZ, UK
(Received 7 January 1991; accepted 28 February 1991)

The morphology of crystallites in a low molecular weight copolymer of 1,4-oxybenzoate and 2,6-oxynaphthoate units is investigated with transmission electron microscopy (TEM), scanning electron microscopy (SEM) and small-angle X-ray scattering. Selected-area electron diffraction patterns exhibit aperiodic meridional maxima, indicating random sequencing of units along the chains, while sharp equatorial reflections suggest some level of crystallinity. Strongly diffracting crystalline entities, whose number and dimensions depend on thermal history, can be imaged in dark-field TEM. They orient with their thin axis parallel to the molecular director. Similar crystallites are also observed in SEM micrographs of chemically etched bulk samples, and give rise to a small-angle reflection on the meridian of an X-ray fibre pattern. The reflection corresponds to the mean distance between crystallite centres. Crystal thicknesses determined from mean crystallite spacings and percentage crystallinities (measured from wide-angle X-ray scattering) are compared with predictions for various models. The data clearly indicate lateral register between aperiodic sequences, which is the basis of non-periodic layer crystallites.

(Keywords: NPL crystallite; liquid crystalline polymers; thermotropic random copolymers; electron microscopy; small-angle X-ray scattering)

INTRODUCTION

Characteristics of crystalline entities in a series of high molecular weight thermotropic copolymers composed of 1,4-oxybenzoate (B) and 2,6-oxynaphthoate (N) monomer units have recently been determined with the use of dark-field imaging in transmission electron microscopy (TEM)[1]. These crystallites, which are similar to those first reported by Donald and Windle[2], appear to be no more than 20 nm thick and 40–80 nm long, the measured average values depending on the molecular composition and thermal history. They are oriented with their thin axis parallel to the molecular director. Since the B–N copolymers studied possess random intramolecular sequencing, as determined from the presence of aperiodic meridional maxima in both electron[1,3] and X-ray[4–7] diffraction patterns, and from n.m.r. sequencing[8], the existence of ordered entities has been interpreted in terms of registration between identical although aperiodic monomer sequences on adjacent chains. The resultant ordered regions are known as non-periodic layer (NPL) crystallites[9].

This paper focuses attention on a low molecular weight (LMW) variant of B–N ($M_n \simeq 5000$) which also displays crystalline ordering. Results obtained from TEM[1,10] and scanning electron microscopy (SEM)[7,10,11] have revealed that the crystallites in this particular material are up to 10–15 nm thick and up to 300 nm long. Wide-angle X-ray scattering (WAXS) studies[7,12] have shown that annealing above the glass transition temperature (T_g) in the solid state results in an increase in crystalline order. This increase is significantly greater than that seen in high molecular weight ($M_n \sim 30\,000$) analogues subjected to the same thermal treatment.

The object of the present work is to characterize the morphology and dimensions of the crystallites formed in a single LMW B–N copolymer, using the techniques of TEM, SEM and small-angle X-ray scattering (SAXS), combined with crystallinity measurements from WAXS. Comparisons are drawn between the dimensions obtained using the different techniques, and the data are interpreted in the context of various models of crystal structure.

EXPERIMENTAL

Materials. The copolymers used in this study were provided by the Hoechst-Celanese Corporation (Summit, New Jersey, USA). The chemical nature of the monomer units is well-established in the literature[1,3,5–8] and is not reproduced here. Suffice it to say that the copolymers are synthesized from 75 mol% 1,4-hydroxybenzoic acid units and 25 mol% 2,6-hydroxynaphthoic acid units. A material with a low average degree of polymerization (*DP*), of ~25, is the main subject of study (LMW B–N). Where comparison is drawn to the high molecular weight (HMW) copolymers, which have a *DP* of ~150, they are designated HMW B–N.

Sample preparation. Since both TEM and SEM were used to image the crystallites in this study, two entirely different sample preparation techniques were employed. To obtain electron-transparent ultrathin films ($\leqslant$100 nm

* Current address: Strategic Planning Associates, 1 Grosvenor Place, London SW1, UK
† Current address: The Procter & Gamble Company, Miami Valley Laboratories, Cincinnati, OH 45239-8707, USA
‡ To whom correspondence should be addressed

0032-3861/92/010003-08

thick) for use in TEM, a melt-shearing procedure[1] was used. As-received pellets of the copolymer were cut into small blocks. Each block was then heated on freshly cleaved rocksalt to 310°C (unless otherwise stated), which is above the temperature at which LMW B–N enters into its fluid mesophase (~286°C*). The molten copolymers were sheared across the substrate with a razor blade at this temperature (T_s); and after being quenched to 0°C on an aluminium block, the resultant films were floated off the rocksalt substrate in distilled water. The films, picked up on folding copper TEM grids, were annealed for predesignated times (t_a) at specified temperatures (T_a), with long-term anneals performed in an inert atmosphere. All films were subsequently carbon-coated to improve stability under the electron beam.

The method of producing samples for SEM, presented in detail elsewhere[11], relied on capillary spreading of molten copolymer (heated to 340°C) between glass slides to yield uniformly thick films of the order of 5 μm or so. Each specimen was then quenched, annealed at T_a for a time t_a, and then quenched again. The glass slides were then split apart in liquid nitrogen, and the film surface was subjected to a chemical etch consisting of 2 wt% $KMnO_4$ in *o*-phosphoric acid, which preferentially attacked the amorphous matrix, leaving behind surface relief due to the crystalline structure[11]. To improve stability under the electron beam, the SEM samples were then lightly coated (~20 nm) with Au–Pd.

Samples used in the WAXS analyses were similar to those prepared for SEM. The copolymer was spread in its fluid mesophase at 340°C onto a silicon wafer and was then quenched, annealed, quenched again and analysed. Crystallinities were determined by initially subtracting the incoherent scattering and then determining the distribution of scattering intensity between the crystalline and amorphous parts of the diffraction pattern.

Samples used in the SAXS analyses were prepared from fibres drawn from molten pellets at ~315°C. The fibre diameter was typically 0.5 mm. The fibres were annealed and then assembled into a flat parallel array supported on a card frame for use in the small angle camera.

Instrumentation. The electron microscope from which TEM micrographs were obtained was a Jeol JEM 2000-EX, fitted with a LaB_6 filament and a high-resolution pole-piece and operated at 200 keV (to reduce the extent of radiation damage suffered by the organic crystals). Microdensitometry of resulting micrographs was performed using a Joyce-Loebl digital scanning microdensitometer (Technical Operations Inc., Burlington, MA, USA) and resulting images, measuring 512 × 512 pixels, were enhanced with the application of a high-pass filter (Semper VI algorithm by Synoptics Ltd). High-resolution SEM micrographs were acquired with a Cambridge Instruments S-2 microscope, operated at 30 keV and focused with the image-store accessory.

A Siemens θ–θ diffractometer, fitted with a temperature-controlled furnace (±5°C accuracy), was employed to record wide-angle X-ray traces from 10 to 40° 2θ with CuKα radiation. Each scan required ~12 min. The small-angle camera employed Kratky collimation and a Braun quartz-fibre position-sensitive X-ray detector (PSD). Samples were mounted with the fibre axis either parallel or perpendicular to the PSD yielding meridional or equatorial scattering curves, respectively. The data presented are preliminary results which have not had backgrounds subtracted or been desmeared to take account of the beam profile. Each exposure took 8 h.

* Obtained by d.s.c. operated at 20°C min^{-1} in a nitrogen atmosphere

THE NPL MODEL OF CRYSTALLINITY

The essence of any model of copolymer crystallization of extended chain polymers is the lateral registration of monomer sequences. Flory[13] considered the situation in which the polymers consisted primarily of crystallizable monomer units with just a small proportion of non-crystallizable units. Crystals were formed by a segregation of homopolymer sequences, which occur at random along the chains, with the non-crystallizable units being effectively excluded from the crystals. The concentration of non-crystallizable units governed the lengths of homopolymer sequences available, and hence the distribution of crystallite sizes.

The NPL model differs from the Flory theory in that it describes crystallites which are based on lateral register between similar, yet aperiodic, monomer sequences of neighbouring molecules of a random copolymer. It was formulated[9] to take account of the results of diffraction studies of thermotropic random copolyesters which showed crystalline order which was not based on homopolymer sequences; the aperiodicity in the chain direction was somehow propagated laterally so that the characteristic aperiodic meridional diffraction maxima were concentrated onto the meridional axis rather than appearing as extended layer lines.

We may consider four different cases of random copolymer crystallization which vary in the degree of lateral registration that is present.

1. Plane start registration. This is lateral registration in which one point on one monomer unit on each chain is in register. In the present case, the point might be the ester group which is common to both monomer units. There is no sorting of the comonomer sequences, however, so that the register is not maintained in the chain direction. The model has been discussed previously by Biswas and Blackwell[14] and by Golombok *et al.*[15]. It is effectively forced register within a single plane (*Figure 1a*), the register not involving any relative movement of the molecules greater than the lengths of the monomer units. Plane start registration has been assumed to occur[14], without the need for annealing, at random points throughout the polymer matrix. The register decays on moving away from the plane of registration. There is thus a partially ordered fringe region above and below the plane of registration, in which there is imperfect sequence matching on adjacent chains, but which must contribute to the crystallinity in some way. In the context of NPL crystallites, the plane start may be thought of as possessing the minimum possible degree of registration.

2. Cold crystallization. This case is based on the model of Wunderlich[16]. There will be, by chance, regions within the polymer in which similar sequences of units are positioned beside each other, making small NPL crystallites without the need for segregation over distances greater than the length of one monomer unit. This type of NPL crystallite might also be thought of in terms of plane start registration which occurs within

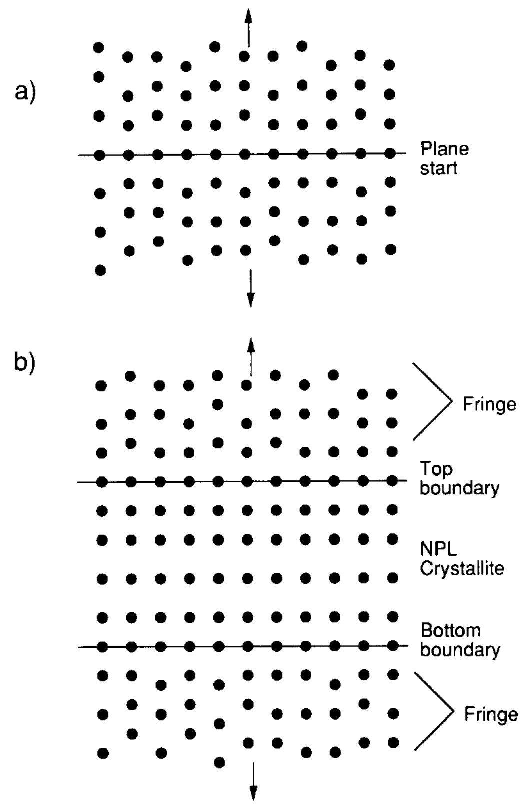

Figure 1 (a) Schematic representation of the plane start model of copolymer crystallinity. The diagram shows a section through a crystallite perpendicular to the plane of registration. The ester groups on the B and N units are represented as dots. (b) Section through an NPL crystallite showing the fully ordered core and partially ordered fringe regions

favourable regions of the polymer where there is already some degree of sequence matching. Cold crystallization registration is thus a development from the plane start model, and will include regions of partial order above and below the crystal along the polymer chain.

3. Aperiodic sequence segregation. This arrangement represents a development of cold crystallization register in which the thickness of the NPL crystallites is enhanced by a relative longitudinal motion of the molecules, during annealing, over distances up to the length of the whole chain. The motion can be thought of as a searching process, the effect of which is to increase the lengths of aperiodic sequences which can come into register, and hence the thickness of crystallite along the chain direction. Once again we would expect the effective dimensions of the crystallite to be further enhanced by partially ordered fringe regions above and below the crystallite along the chain direction (*Figure 1b*).

4. Homopolymer segregation. This arrangement again involves segregation, but in this case it is the homopolymer sequences which occur by chance within the random copolymer molecules, which are segregating and crystallizing as in the Flory model. The crystals formed will be conventional regular homopolymer ones, albeit thin, and not NPLs. However, we may note that even a homopolymer crystal will possess a partially ordered fringe region.

The four crystallization regimes described above have been studied using computer models and statistical analysis[12,17] in order to evaluate the limits on crystallite size and percentage crystallinities in each case. The results for a three-dimensional model containing chains of 25 monomer unit length are summarized in the first column in *Table 1*. In the annealed models, segregation of sequences has been permitted over distances up to ± 25 monomer units in the chain direction. We can see that the best homopolymer crystals that are likely to form during annealing will be little longer than the NPL crystallites that form in a quenched system (2.5–3.0 nm). However, the best NPL crystallites formed on annealing are $\sim$4.4 nm long.

The partially ordered fringe region has been shown, through modelling of its autocorrelation function[15], to decay relatively slowly, and to extend over a region of up to $\sim$5 nm from the plane start or crystal boundary. It has also been shown from diffraction simulations[14,15] that a plane start can generate sufficient ordering to produce sampling of layer lines on the meridian of the fibre pattern. If we compare the meridional intensities for a plane start model with those from perfect NPL crystallite models, we find that the fringe diffracts in an equivalent manner to a perfect NPL crystal with no fringe of three to four unit thickness along the chain direction. If we include this contribution from the fringe in the dimensions of the crystallites, taking care not to count the boundaries twice in the calculation, we obtain the results shown in the second column in *Table 1*. The dimensions quoted are equivalent sizes of perfect crystals, and so may be correlated with values obtained below using percentage crystallinities which are calculated on the assumption of perfect crystals. It is interesting to note that the upper limit on the equivalent dimension of a plane start crystallite ($\sim$4.1 nm) is roughly half what may be obtained for an annealed NPL crystallite ($\sim$7.8 nm), with the other models having intermediate dimensions. Thus, by measuring the crystal dimensions experimentally, it should be possible to distinguish between the models presented above, and to determine whether the order observed is due to large scale segregation into crystals or minimal segregation to give a plane start.

DIMENSIONS FROM TEM AND WAXS CRYSTALLINITY MEASUREMENTS

Direct observation. Figure 2a shows an electron diffraction pattern obtained from a sample of LMW

Table 1 Crystal thicknesses parallel to the long axis of the polymer molecules, as predicted by computer simulation, for B–N chains of 25 monomer unit length, and composition 75:25

	Crystallite thickness (nm)	
	No fringe	With fringe
NPL quenched	2.53 ± 0.10	5.93 ± 0.43
NPL annealed	4.38 ± 0.18	7.78 ± 0.45
Homopolymer annealed	2.88 ± 0.12	6.28 ± 0.43
Plane start	–	4.08 ± 0.41

The first column shows the thickness of the crystallite alone, while the second column includes the equivalent dimension of the fringe region (see text). In accounting for the fringe, care was taken to count the monomer units at the boundaries between the crystal and the two fringes once only. Thus the length of two monomer units was deducted from the total length of the crystals. The plane start was treated differently: the length of one monomer unit was deducted, to avoid counting the plane of registration twice

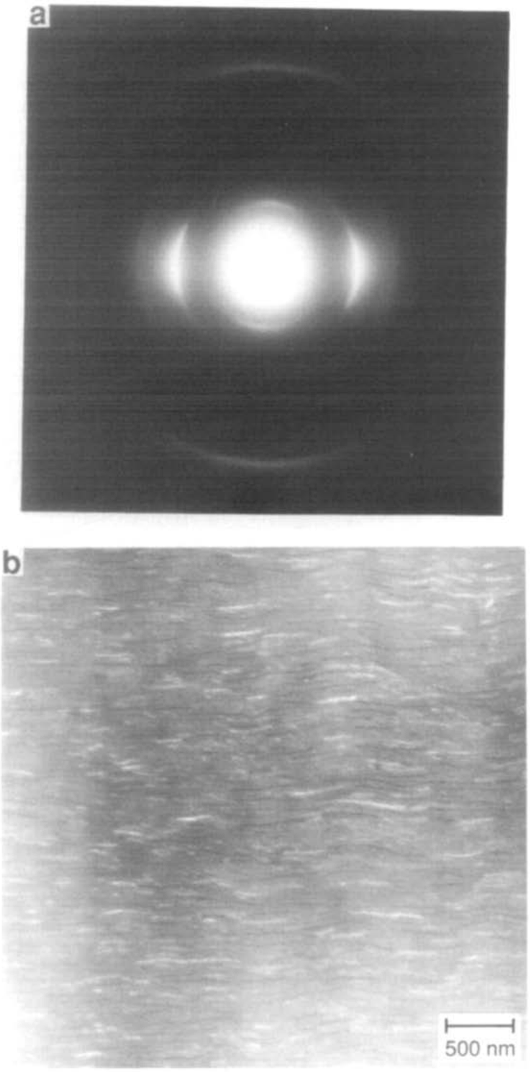

Figure 2 (a) Typical selected-area electron diffraction pattern of the LMW B–N thermotropic copolymer, obtained from a region measuring $\sim 2.5\ \mu m$ in diameter. Aperiodic meridional maxima indicate random intramolecular sequencing, and sharp reflections suggest the presence of finite crystallinity. (b) Dark-field image of LMW B–N as imaged in the principal equatorial reflection. The micrograph clearly shows the presence of crystallites, measuring ~ 10–15 nm thick and up to ~ 300 nm long and oriented with their short axis parallel to the molecular director (vertical)

B–N. The principal features are strong equatorial maxima and aperiodic meridional maxima. *Figure 2b* is a dark-field electron micrograph of LMW B–N imaged in the principal equatorial reflection, which is the approach used in most of the NPL crystallite observations so far[1–3,10]. The sample was sheared at 200°C, and annealed at the same temperature for 30 min. While some of the crystallites are oriented so that they diffract into the objective aperture and appear brighter than the background, many diffract outside the aperture and are darker than the background. It should also be pointed out that all of the crystallites are oriented with their thin axis parallel to the molecular director, which in this as well as all subsequent TEM micrographs, is vertical on the page.

The crystallites in *Figure 2b* appear ~ 10–15 nm thick but it must be kept in mind that TEM gives a projected view, and thus will exaggerate the true thickness in circumstances where the platelets are neither exactly edge on to the beam nor precisely flat with uniform thickness. Thus the thickness mentioned above must be seen as an upper limit. The lateral length dimension of the crystallites in the specimen plane, known as the crystal length, is 250 ± 70 nm. This value[1] is considerably greater than that for HMW B–N in which case the mean length is 50–70 nm. The shape of the crystallites appears to be quite irregular, as seen in a digitized image (*Figure 3*) obtained from an area of *Figure 2b* and enhanced with the application of a high-pass filter. This image shows that the top and bottom interfaces of the crystallites are far from smooth. The mean spacing between the crystal centre lines in the direction of the molecular chain axes is 39 ± 3 nm. The reliability of this measurement depends on the lateral dimensions of the crystallites in the direction normal to the film being at least of the same order as the film thickness (~ 100 nm). In the present case the crystal length in the specimen plane is much greater than this value, so the assumption is reasonable.

Tilting the electron beam so that the third meridional arc is centred in the objective aperture produces the

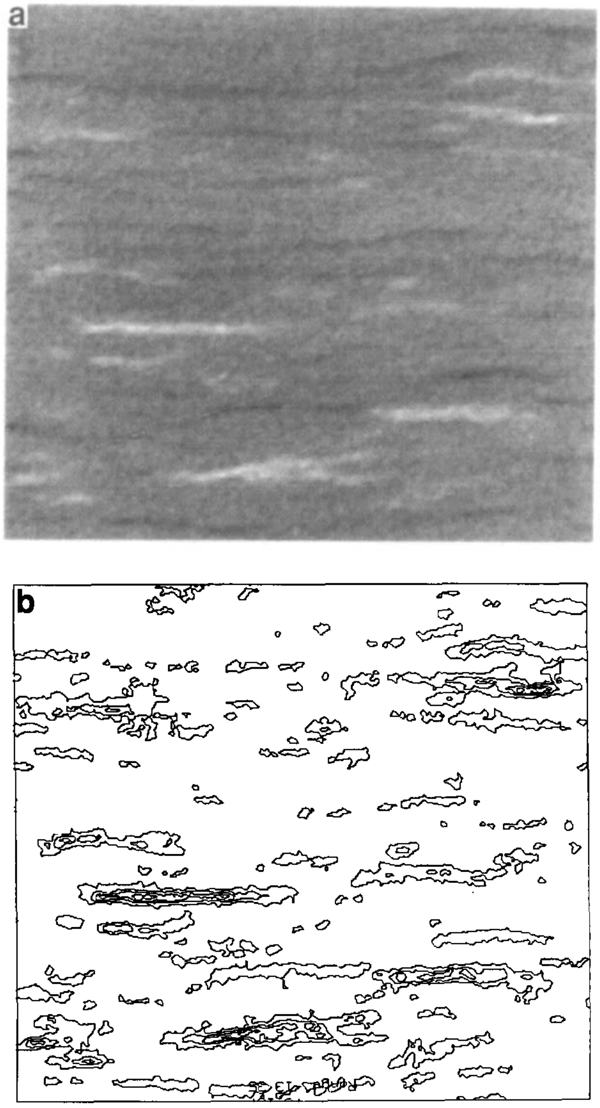

Figure 3 Digitized enlargements of a region of the micrograph in *Figure 2b*. The features in (a) have been enhanced with the application of a high-pass filter. The corresponding contour map (b) illustrates the non-uniform, ragged edges of these crystallites

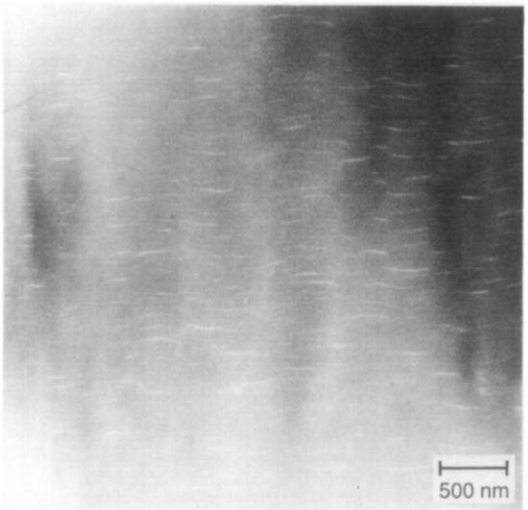

Figure 4 Dark field micrograph of LMW B–N as imaged in the third meridional arc of the electron diffraction pattern. The crystallites appear similar to those seen in *Figure 2*. Imaging in any of the meridional reflections has not been successful with HMW B–N materials due to radiation sensitivity and the lack of diffraction intensity

dark-field micrograph presented in *Figure 4*. Crystallites are visible in this imaging geometry and measure ~15 nm thick and ~190 nm long. No crystallites are observed in corresponding images from HMW B–N. Imaging has not been successful in the first meridional arc of any B–N copolymers, due to lack of diffraction intensity coupled with rapid beam damage, but crystals have been observed when imaged in the first or third meridional reflections in a chemically related copoly(ester-amide)[18]. The mean spacing in this micrograph (*Figure 4*) is 50 nm, although as crystallite visibility is rather more marginal than for the equatorially imaged micrograph, it is possible that this value might be an overestimate.

The dimensions of the crystallites determined from the TEM micrographs are summarized in *Table 2*.

Crystal thickness using WAXS crystallinity. As discussed above, the direct TEM measurements of crystal thickness must be considered as upper limit values. In view of the importance of this parameter in distinguishing between models for crystal structures, another approach has been used based on the rather more reliable mean spacing obtained from the micrographs, and the crystallinity (χ) measured from WAXS scans. The values of crystallinity are given in *Table 3*, measured both at various annealing temperatures and after quenching from those temperatures. Thus, the specimens examined by TEM can be considered to have a crystallinity of ~19%. These values are in line with estimates of 21% made on higher molecular weight materials with composition[19] 40:60, but significantly less than the 30–60% (depending on thermal history) reported for materials with 58:42 composition[20].

Assuming that the lateral dimensions of the crystallites perpendicular to the film are at least as great as the film thickness, we can find the crystallite thickness (Θ) from the crystallinity (χ) using:

$$\chi = \frac{\Theta}{d} \times 100\%$$

where d is the mean spacing of the crystallites. Hence the estimate of thickness is 7.4 ± 1.1 nm. This value is less than the upper limit of thickness obtained by direct measurement, of 10–15 nm. The calculated value is also an upper limit, for if the crystallites are uniformly tilted so that their thin axes make an angle α to the plane of the film, the mean spacing measured would be overestimated by a factor of $\sec \alpha$, and the thickness would be overestimated by the same amount. However, this effect will be very small compared with the influence of small tilts on the projected thickness, where the apparent increase in thickness is proportional to $\sin \alpha$, and depends on the ratio of specimen thickness to crystal thickness.

DIMENSIONS OF CRYSTALLITES REVEALED BY ETCHING

Observations of etched surfaces. Figure 5 shows a series of scanning electron micrographs of etched longitudinal fracture surfaces of split polymer films. The platelet-like morphology of the crystals is again apparent. The heat treatments to which the polymers were subjected prior to examination are listed in the micrographs, and in these figures the molecular chain axis is horizontal. In *Figure 5a* the heat treatment is at a sufficiently low temperature to have little influence on the crystallite sizes, compared with the sample cooled from the melt. The mean dimensions for each case are listed in *Table 4*. Note that for the two modest anneals (170 and 215°C) the mean spacings, 41.0 and 40.2 nm, are very similar to that determined from TEM (39 nm). The mean length of the crystallites, for the lightly annealed sample (*Figure 5a*) is 270 nm, again of the same order as observed in TEM.

Table 2 Crystallite dimensions observed from TEM micrographs of LMW B–N, sheared at 200°C and annealed at that temperature for 30 min

Imaging mode	Mean spacing (nm)	Thickness (nm)	Length (nm)
Equatorial	39 ± 3	12 ± 2	250 ± 70
Third meridional	50 ± 3	15 ± 2	190 ± 50

Table 3 Percentage crystallinities (χ) measured from WAXS for samples of LMW B–N, at the temperature of anneal (T_a) and after quenching to room temperature

T_a (°C)	t_a (h)	χ at T_a (%)	χ after quench (%)
170	12	18 ± 2	18 ± 2
200	1	20 ± 2	19 ± 2
215	4	18 ± 2	22 ± 2
260	2	10 ± 1	20 ± 2
290	2	6 ± 1	14 ± 1
350	0.05	0	14 ± 1

Table 4 Crystallite dimensions as observed on etched specimens of LMW B–N by SEM

T_a (°C)	t_a (h)	Mean spacing (nm)	Thickness (nm)	Length (nm)
170	5	41.0	18	270
215	2	40.2	23	152
260	2	56.0	26	250
290	1	154	34	350

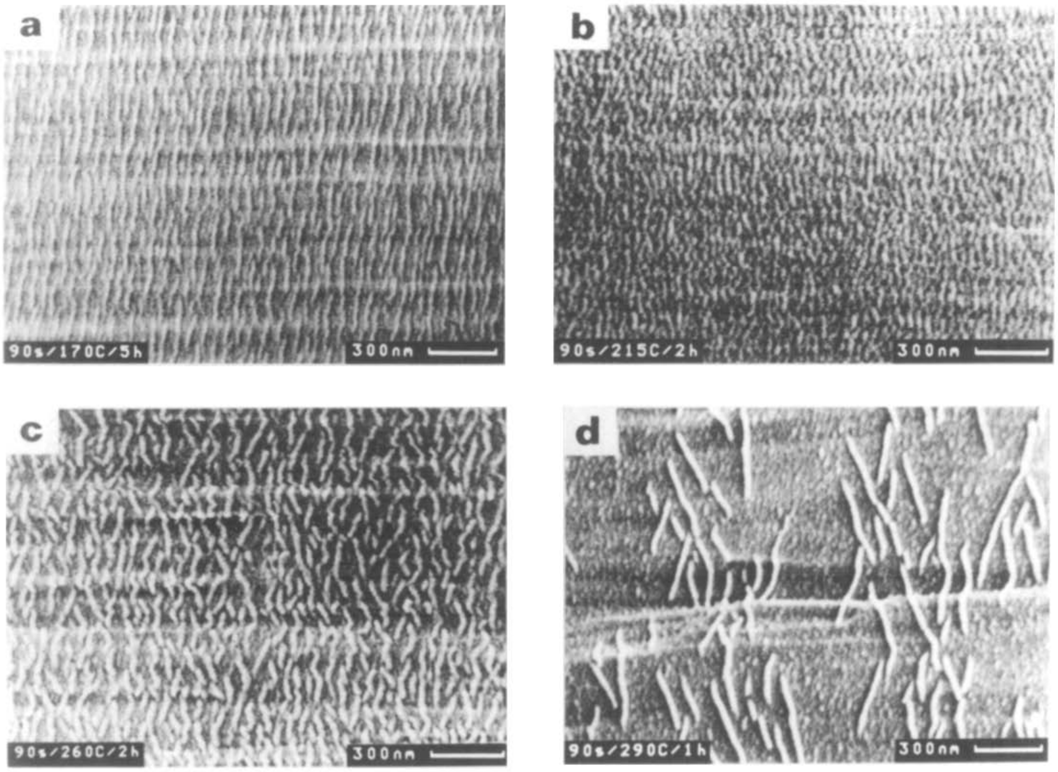

Figure 5 SEM micrographs of chemically etched LMW B–N showing the effect of annealing temperature on the morphology of NPL crystallites. In each case, the numerical designation in the lower left corner provides processing information in the form of etching time/annealing temperature T_a (°C)/annealing time t_a (h). The parameter to which attention is drawn in this series of images is T_a: 170°C in (a), 215°C in (b), 260°C in (c) and 290°C in (d). Unlike the TEM images, the molecular director in these micrographs is horizontal

The crystal thicknessses are difficult to assess accurately as they are not clearly defined on this size scale. This is especially true in the case of the sample annealed at 215°C (*Figure 5b*), which has been etched rather more deeply. It is also likely that the rather shorter crystal length in this case is due to etch-induced discontinuities along the crystallites. As with the TEM observations, but for rather different reasons, it is not clear how accurately the apparent crystal thickness represents the actual thickness. It is interesting, however, that the mean value does tend to increase with increasing annealing temperatures.

Before considering the higher temperature treatments, it is worth noting that the combination of mean spacing and crystallinity also gives a crystal thickness in the region of 7–8 nm, in close agreement with the value obtained from TEM mean spacing.

Effect of anneals at 260°C and 290°C. Figures 5c and *d* show an increase in crystallite dimensions as a result of annealing. There is a distinct increase both in mean spacing and apparent thickness. In the sample annealed at 290°C, which is very close to the melting point, there has been a very marked coarsening of the structure. The crystallinity at the annealing temperature also appears very much lower, the apparent increase in thickness in no way compensating for the increase in spacing. From *Table 3*, the measured crystallinity at 290°C is 6%, and it is clear that the small proportion of crystals which had not melted out at that temperature are the ones which have coarsened so dramatically in *Figure 5d*. On quenching from 290°C further crystals formed, the measured crystallinity at room temperature being 14%, but these are small and finely distributed within the matrix as can be seen in *Figure 5d*. The fact that the crystallites appear to assume a bimodal orientation distribution about the orientation axis in *Figures 5c* and *d*, is not yet understood. It may represent a different crystal habit associated with the crystal structure transformation from pseudo-hexagonal to orthorhombic which occurs on annealing[12,21,22], or it might be associated in some way with a relaxation of the orientation in the matrix. It is also apparent that the large crystals are thicker than could readily be accounted for by the segregation of matched units. It is possible that, in this case, a degree of chemical rearrangement may be involved.

It was not possible to develop similarly coarsened structures by annealing thin films suitable for examination by TEM. This is thought to be due to the restrictions on molecular organization imposed by the thinness of the film. The structures obtained in extensively annealed bulk (5 μm thick) specimens are on a scale much larger than the TEM specimen film thickness.

SMALL ANGLE X-RAY SCATTERING

While there is conclusive evidence for the existence of crystallites in these polymers, it is noteworthy that as-drawn fibres exhibit a SAXS trace, as in *Figure 6a*, which is devoid of the discrete maxima one might expect from stacks of crystalline lamellae. Such observations are in line with several earlier reports for higher molecular weight examples of similar materials[23]. However, it is observed that if a drawn fibre is annealed under conditions which are sufficient to induce a phase transition from pseudo-hexagonal to orthorhombic[12,21,22] without

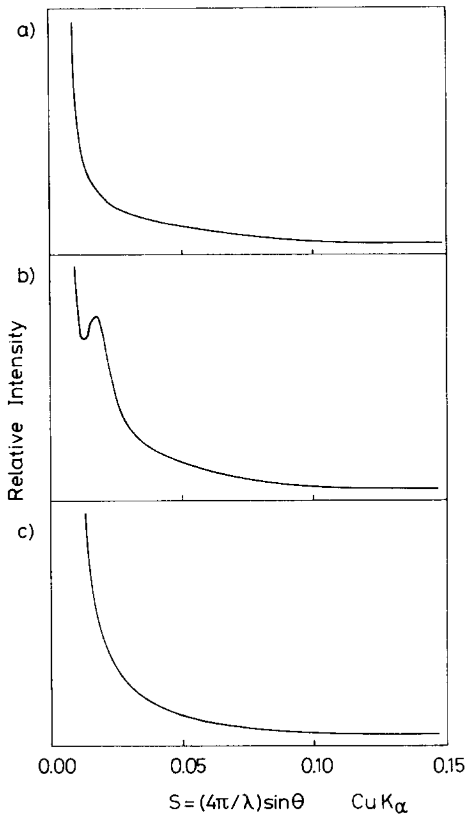

Figure 6 Meridional SAXS curves from LMW B–N for (a) as-drawn fibres, (b) fibres annealed for 1 h at 215°C and (c) fibres annealed for 1 h at 290°C

markedly coarsening the structure, in this case at 215°C for 1 h, then a small angle peak appears as can be seen in *Figure 6b*. It corresponds to a long period of 35.5 ± 0.5 nm in a direction along the fibre axis and thus normal to the lamellae.

The lack of small angle peaks in the unannealed material is a consequence of the similarity of the densities of the metastable pseudo-hexagonal crystal phase, which forms first on cooling and the surrounding non-crystalline matrix. The formation of the equilibrium orthorhombic phase on annealing has been discussed elsewhere[22]. Its density is 6% greater than that of the metastable pseudo-hexagonal phase and the resulting contrast is sufficient to give the SAXS peak.

A sample annealed for 1 h at 290°C shows no peak (*Figure 6c*). Such an observation is not surprising, since *Figure 5d* indicates that the structure is sufficiently coarsened after this treatment to put the long period (154 nm from the micrograph) beyond the resolution of the small angle camera.

A series of fibres drawn from HMW B–N of the same composition revealed no SAXS maxima even after 6 h at 210°C. Although further studies are in hand, it may be that the transformation to the orthorhombic phase is sufficiently slowed to prevent the appearance of the peak, at least under the annealing conditions used so far.

DISCUSSION

The long period measured by SAXS (35.5 nm) is somewhat smaller than the mean spacing of the crystals obtained either by TEM (39 nm) or SEM of etched fracture surfaces (41 nm). A possible explanation for this modest anomaly is apparent from the procedure used in determining the mean spacing. When counting the number of intersections per unit length made by crystallites on a line along the molecular axis, it was apparent that a marked regularity in spacing occurred. However, there were often gaps in this sequence where, although a crystallite might be expected, none was seen or counted. Thus the measured mean spacing increased. The effect of missing crystallites on the long period might be to reduce the intensity of the SAXS peak, but not to move it to lower angles corresponding to an increased spacing. The question of whether a proportion of crystallites present in the microscope specimens was not seen or whether all were picked up must remain open at this stage. For this reason, the best value for the mean spacing of the crystallites is taken as the average of the values obtained by the three independent techniques: 38.5 nm.

This revised value for the mean spacing of the crystallites leads to a new value for the crystal thickness of 7.3 ± 1.1 nm. Referring to *Table 1*, we see that the measured thickness is too great to be accounted for by plane start register alone, and is somewhat higher than the maximum dimension obtainable from a homopolymer crystal. Indeed, the value falls very close to that obtained for an NPL model with full chain searching, i.e. maximum anneal. It would be wrong, however, to read too much into the apparent precision of this agreement. There are discrepancies in the figures for mean crystallite spacing given by the different methods, and errors involved in computing crystallinities which, together, lead to at least a 15% uncertainty in the final figure for thickness. Also, the exact equivalent thickness of the partially ordered fringe region is open to some question, for the method of determining the fringe thickness, from diffraction simulations, gives an uncertainty of about half a monomer unit and it is not clear whether the fringe will have the composition of the NPL crystal or the polymer matrix, or some intermediate value, which leads to an uncertainty of ± 0.25 nm in the thickness. However, within the errors indicated, there is clear evidence that crystallinity occurs in the form of NPL crystallites, with the corollary that plane start register alone is incapable of producing the crystallites we have observed.

CONCLUSIONS

The morphology of NPL crystallites in a LMW B–N thermotropic copolyester has been investigated with both TEM and SEM. Crystallites are clearly visible in dark-field electron micrographs imaged in either the principal equatorial reflection or in the third meridional arc. The dimensions of the crystallites depend on the conditions under which the ultrathin TEM films were produced and are typically of the order of 10–15 nm thick and up to ~300 nm long in films subjected to annealing. In unannealed films, the crystallites are fewer and less distinct in appearance. Crystallites are also seen in SEM micrographs of chemically etched copolymer surfaces. Annealing at different temperatures results in a marked change in crystallite morphology, with crystallites becoming much longer and more widely spaced under the higher temperature anneals. A long period is observed by SAXS and corresponds to the spacing between crystallites. It is only observed after modest anneals; for once the structure coarsens, the crystallite spacing passes beyond the lower angular limit of the small angle camera. The long period measured from SAXS is in reasonable agreement with direct measurements from TEM and SEM images.

The average spacing between crystallites for samples annealed at ~200°C for 1 h from all three methods is 38.5 nm and the percentage crystallinity obtained from WAXS measurements is ~19%. Together, these figures yield a crystal thickness of ~7.3 nm, which is close to the maximum dimension expected from modelling of NPL crystallites (7.8 nm) and almost double the dimension expected for a plane start model (4.1 nm), lending strong support to the proposition that crystallinity in random copolymers of 1,4-oxybenzoate and 2,6-oxynaphthoate can only be accounted for by segregation of monomer sequences into crystallites, and cannot be explained on the basis of a plane start model.

ACKNOWLEDGEMENTS

The authors would like to thank the Hoechst-Celanese Corporation for providing the copolymers and for partially funding this project. Sincere gratitude is extended to Professor A. Howie, FRS, and the Microstructural Physics Group (Cavendish Laboratory) for the use of the electron microscope, Professor D. Hull, FRS, for the provision of laboratory facilities, Dr O. Saxton for assistance in image processing, and the SERC for a grant. We would also like to thank Ms E. Bedford for assistance with analysis of the transmission electron micrographs, and one of us (SH) would like to thank Trinity College, Cambridge, for a Senior Rouse Ball Studentship.

REFERENCES

1 Spontak, R. J. and Windle, A. H. *J. Mater. Sci.* 1990, **25**, 2727
2 Donald, A. M. and Windle, A. H. *J. Mater. Sci. Lett.* 1985, **4**, 58
3 Donald, A. M. and Windle, A. H. in 'Recent Advances in Liquid Crystalline Polymers' (Ed. L. Chapoy), Elsevier Applied Science, New York, 1987, Ch. 12
4 Mitchell, G. R. and Windle, A. H. *Colloid Polym. Sci.* 1985, **263**, 230
5 Gutierrez, G. A., Chivers, R. A., Blackwell, J., Stamatoff, J. B. and Yoon, H. *Polymer* 1983, **24**, 937
6 Chivers, R. A., Blackwell, J. and Gutierrez, G. A. *Polymer* 1984, **25**, 435
7 Lemmon, T. J., Hanna, S. and Windle, A. H. *Polym. Commun.* 1989, **30**, 2
8 Economy, J., Johnson, R. D., Lyerla, J. R. and Mühlebach, A. in 'Liquid-Crystalline Polymers' (Eds R. A. Weiss and C. K. Ober), American Chemical Society, Washington, DC, 1990, Ch. 10, p. 130
9 Windle, A. H., Viney, C., Golombok, R., Donald, A. M. and Mitchell, G. R. *Faraday Discuss. Chem. Soc.* 1985, **79**, 55
10 Windle, A. H., Dong, Y., Lemmon, T. J. and Spontak, R. J. in 'Frontiers of Macromolecular Science' (Eds T. Saegusa, T. Higashimura and A. Abe), Blackwell Scientific Publications, London, 1989, pp. 345–348
11 Lemmon, T. J. *PhD Thesis* University of Cambridge, 1989
12 Hanna, S. *PhD Thesis* University of Cambridge, 1988
13 Flory, P. J. *Trans. Faraday Soc. No. 390* 1955, **51**, 848
14 Biswas, A. and Blackwell, J. *Macromolecules* 1988, **21**, 3152
15 Golombok, R., Hanna, S. and Windle, A. H. *Mol. Cryst. Liq. Cryst.* 1988, **155**, 281
16 Wunderlich, B. *J. Chem. Phys.* 1958, **29**, 1395
17 Hanna, S. and Windle, A. H. *Polymer* 1988, **29**, 207
18 Spontak, R. J. and Windle, A. H. *Polymer* 1990, **31**, 1395
19 Blundell, D. J. *Polymer* 1982, **23**, 359
20 Butzbach, G. D., Wendorff, J. H. and Zimmermann, H. J. *Polymer* 1986, **27**, 1337
21 Kaito, A., Kyotani, M. and Nakayama, K. *Macromolecules* 1990, **23**, 1035
22 Hanna, S., Lemmon, T. J. and Windle, A. H. in 'Polymer Science: Contemporary Themes' (Ed. S. Sivaram), Vol. 2, Tata, McGraw-Hill, New Delhi, 1991, pp. 504–509
23 Viney, C., Mitchell, G. R. and Windle, A. H. *Mol. Cryst. Liq. Cryst.* 1985, **129**, 75